

AN ALTERNATIVE WAY TO PREDICT THE PRESENCE OF CRACKS IN A ROTOR BY STUDYING ITS VIBRATIONAL BEHAVIOUR

Brahim BAKHALED¹, Abdelhamid HADJOUI², Ahmed FELLAH³

The present paper aims to study the effects of cracks on the vibratory response of rotors. A new method, based on the theory of local stiffness decrease in a cracked element as compared to that of an uncracked element, is proposed here in order to predict the presence of a crack in a rotor. The classical version of the finite element method (FEM) is used for modeling the cracked rotor. In addition, a computer program was successfully developed using MATLAB in order to determine the critical frequencies of cracked and uncracked rotors. The variation of the critical frequencies as a function of stiffness reduction was examined, in the cases of open and breathing cracks, with the intention of predicting the presence, nature, and severity level of a crack in the rotor.

Keywords: Rotor; Finite element method; Stiffness; Critical frequency; Open crack; Breathing crack.

1. Introduction

Rotating machines play an essential role in industry. Cracks are among the most common defects encountered in rotating equipment due to its extensive use. Cracking in rotors may cause serious damage to rotating machines. During the last decades, several works have been conducted to study the dynamic behaviour of cracked rotors and to ultimately detect the presence of cracks in rotating shafts for preventing damage that can ultimately lead to system failure. The early detection of cracks in a rotor could potentially avoid serious problems, in addition to the costly repairs of the consequential damages; it also minimizes the risks and dangers employees might be exposed to and ensures their protection and safety.

The presence of cracks in rotational shafts reduces their stiffness, which in turn decreases their natural and critical frequencies. Various theoretical and experimental works have shown that the variation of the eigenfrequencies can be used for the detection of the depth and position of the crack in the rotating shaft. Kirmsher [1] and Thomson [2] were the first to examine the effect of

¹ Phd Student, IS2M Laboratory, University of Tlemcen, Algeria.

e-mail: brahim.bakhaled@student.univ-tlemcen.dz

² Prof., IS2M Laboratory, University of Tlemcen, Algeria. e-mail: hadjoui_ab@yahoo.fr

³ Phd Student, IS2M Laboratory, University of Tlemcen, Algeria. e-mail: fellah-gim@hotmail.fr

discontinuities on the natural frequency of beams and bars. Irwin [3] analyzed the stresses and strains in the fractured region of a structure.

The transverse open and breathing crack models are the most common approaches used to simulate the behaviour of a rotating shaft with a crack. Wauer [4] conducted a literature review on the state of the art of cracked rotor dynamics. For instance, some studies were carried out on cracked rotors by the researchers Davies and Mayes [5]; they investigated the vibrational behaviour of a multi-shaft, multi-bearing system in the presence of a propagating transverse crack and indicated that the opening and closing of the crack in a rotor during rotation had a significant effect on its natural frequencies. Moreover, Chasalevris and Papadopoulos [6], on one side, and Sekhar [7], on the other, investigated the influence of two cracks on the rotating system. Furthermore, Sekhar and Prabhu [8] studied a cracked rotor passing through its critical speeds. Similarly, Sinou [9] conducted a study on the effects of a crack on the stability of a non-linear rotor system.

The most common techniques employed to formulate the stiffness of the cracked element using the FEM are the flexibility matrix method [6-8] and the time-varying stiffness method [9-14]. Based on the time-varying stiffness approach, Sinou and Lees [10] inquired into the influence of the position and depth of a crack on the eigenfrequencies of the system. Al-Shudeifat et al. [11-14] carried out experimental and theoretical studies on the influence of open and breathing cracks on the vibrational behaviour of symmetric and asymmetric rotors, in the case of critical and subcritical harmonics.

The present work attempts, first, to use the classical version of the FEM and the time-varying stiffness method for modeling the cracked rotor. Using a program developed under the software MATLAB, one can easily determine the critical frequencies of cracked and uncracked rotors. The mesh convergence test allows us to fix the number of elements. Then, the results obtained from the previously developed computer program are validated by comparing them with the theoretical and experimental ones reported by Al-Shudeifat [14]; this validation operation is performed in order to evidence the efficiency of our model and the reliability of the developed program. Next, a new method is suggested to predict the presence of cracks in the rotating shaft. This method is based on the concept of stiffness reduction of the cracked element as compared to that of the uncracked element. This stiffness decrease may be expressed by means of a relationship between the cracked element stiffness K_{crack} and the uncracked element stiffness $K_{nocrack}$. This method is intended to study the open and breathing cracks in rotors. From the results obtained by this method, one can create a database that allows predicting the presence of a crack, its nature and its degree of severity.

2. Equation of motion

The rotor consists of a shaft supported by bearings and comprising one or more disks. It may also be subjected to other stresses (loads) such as unbalance or external forces. The equation of motion is obtained from the kinetic and deformation energies of the rotor components and by the application of the Lagrange equation below:

$$\frac{d}{dt} \left(\frac{\partial T}{\partial \dot{q}} \right) - \frac{\partial T}{\partial q} - \frac{\partial U}{\partial q} = F \quad (1)$$

where T and U are respectively the kinetic and potential energies of the system and q represents the generalized coordinates; F represents all external forces.

2.1. Kinetic energy of the disk

The disk is considered as rigid; it is characterized by the kinetic energy that is expressed as:

$$T_d = \frac{1}{2} m_d (\dot{u}^2 + \dot{w}^2) + \frac{1}{2} I_{dx'} (\dot{\psi}^2 + \dot{\theta}^2) + \frac{1}{2} I_{dy'} (\Omega^2 - 2\dot{\psi}\dot{\theta}) \quad (2)$$

where m_d is the mass of the disk, u and w are the horizontal and vertical displacements, respectively, ψ and θ are the angles of rotation around the axes x and z (fixed coordinates), respectively (Figure 1), Ω is the rotational speed, $I_{dx'}$ and $I_{dy'}$ are the moments of inertia of the disk along the axes x' and y' (Figure 1). These may be written as:

$$I_{dx'} = \frac{m_d}{12} (3r^2 + 3R^2 + h^2) \quad , \quad I_{dy'} = \frac{m_d}{2} (r^2 + R^2) \quad (3)$$

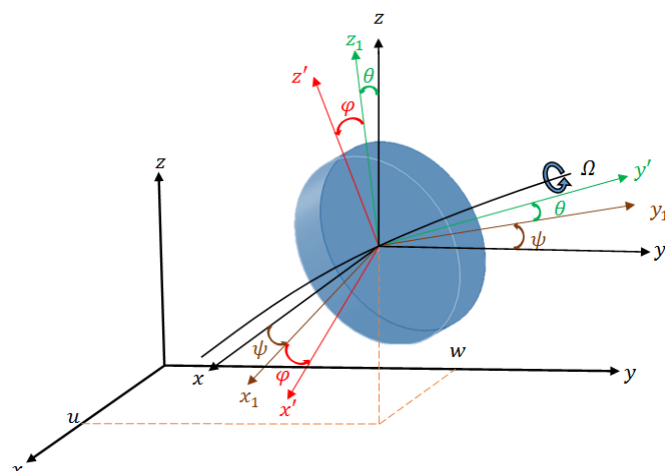


Fig.1. Fixed and rotational coordinates of the disk

2.2. Kinetic and deformation energy of the shaft

The rotating shaft is represented by a beam with a circular cross section. The expression of the kinetic energy of an element of length L is given by:

$$T_a = \frac{\rho S}{2} \int_0^L (\dot{u}^2 + \dot{w}^2) dy + \frac{\rho I}{2} \int_0^L (\dot{\Psi}^2 + \dot{\theta}^2) dy + \rho I L \Omega^2 + 2 \rho I \Omega \int_0^L \dot{\Psi} \theta dy \quad (4)$$

where ρ is the density of shaft material, S and I are the area and moment of inertia of the shaft's cross section, respectively.

In the case of a symmetric shaft's cross section, where $I_x = I_z = I$, the deformation energy may be expressed as:

$$U_a = \frac{EI}{2} \int_0^L \left[\left(\frac{\partial^2 u}{\partial y^2} + \frac{\partial^2 w}{\partial y^2} \right)^2 \right] dy \quad (5)$$

The expressions of I_x and I_z were developed by Al-Shudeifat and Butcher [12] for the case of a cracked element whose shaft's cross section is not circular (asymmetric cross section).

3. Modeling of the cracked rotor

The cracked rotor was modeled by means of the classical version of the Finite element method (FEM).

The shaft was discretized in N Euler-Bernoulli beams (Figure 2); each node in the element had four degrees of freedom (two displacements and two rotations). The disk, which was placed between two elements, at a given node, also had four degrees of freedom (DOFs). The unbalance mass m_e could be placed on one or more disks. This mass was located at the distance d from the rotor center. The bearings which were located at specific nodes were characterized by their virtual works.

The different steps used in modeling, the elementary matrix for each component of the rotor, as well as the matrix of the cracked element, have been clearly presented by Al-Shudeifat et al. [11]. These authors established the equation of motion for the global system as given below:

$$M\ddot{x} + (C_p + G)\dot{x} + (K - K_{crack} + K_p)x = F_{Bal} \quad (6)$$

where M represents the global mass matrix which comprises the mass matrices of the shaft and disk, C_p is the damping matrix of bearings, and G the global gyroscopic matrix of the shaft and disk. Moreover, K is the global stiffness matrix of the shaft and K_{crack} the stiffness matrix of the cracked element, K_p the stiffness matrix of bearings, and F_{Bal} is the vector of unbalance forces.

The natural and critical backward and forward whirling speeds may be determined from the eigensolutions of the matrix S for each value of Ω :

$$S(\Omega) = \begin{bmatrix} 0 & I \\ -M^{-1}(K - K_{crack} + K_p) & -M^{-1}(G + C_p) \end{bmatrix} \quad (7)$$

4. Results and discussion

4.1. Convergence study

In this section, the convergence of the first backward and forward critical frequency of the uncracked rotor is presented; it is obtained by increasing the number of elements N (convergence in the classical version of FEM). The physical parameters of the studied rotor were given by Al-Shudeifat [14] and are summarized in table 1.

Figures 2 and 3 present the convergence curve of the first backward and forward critical frequency of the uncracked rotor under study. These figures indicate that the first backward and forward critical frequency converges starting from 6 elements, in which case the two disks are fixed at nodes 2 and 6, and the unbalance mass is placed on the second disk at node 6. The finite element model (FEM) of the rotor under study is illustrated in figure 4.

Table 1:

Physical parameters of the studied rotor.

Description	Value	Description	Value
Length of the rotor shaft	0.65 m	Number of disks	2
Outer radius of the shaft (R)	0.0795 m	Position of disk 1 from the left bearing	0.108 m
Density of the shaft (ρ)	7800 kg /m ³	Position of disk 2 from the left bearing	0.542 m
Young's modulus (E)	2.1e11 N/m ²	Outer radius of the disks (R)	0.0762 m
Bearing stiffness (K_{xx}, K_{zz})	7e7 N/m	Inner radius of the disk (r)	0.0795 m
Bearing damping (C_{xx}, C_{zz})	5e2 Ns/m	Density of the disks (ρ_d)	2700 kg /m ³
Unbalance mass(m_e)	6.3e-4 kg.m	Mass of the disks	0.571 kg
Unbalance Angle (β)	$\pi/2$ rad	Thickness of the disks	0.01172 m

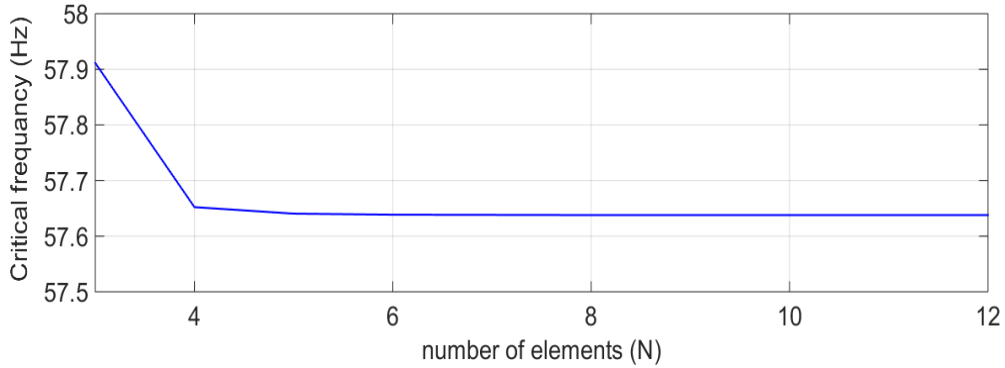
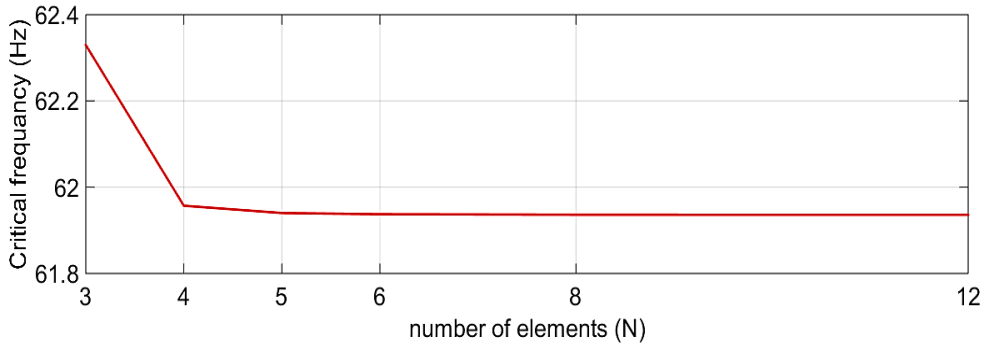
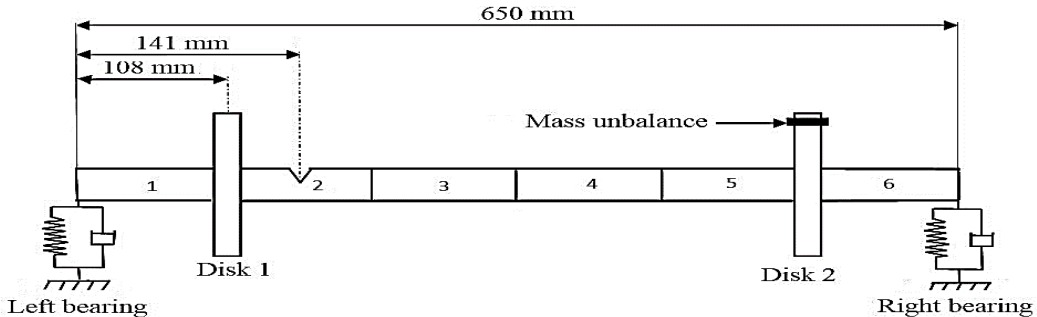
Fig. 2. Convergence curve of the first critical backward frequency (ω_{b1})Fig. 3. Convergence curve of the first critical forward frequency (ω_{f1})

Fig. 4. Finite element model of the studied rotor.

4. 2. Validation

The validation is carried out to confirm the efficiency of our modelling and the reliability of our program. Tables 2 and 3 show the deviation (ε) between the values of the first three backward and forward critical frequencies of uncracked and cracked rotors obtained by the program developed in this study and the theoretical and experimental results reported by AL-Shudeifat [14], where the

crack is located in the second element (Figure 4). The deviations between our results and those of Al-Shudeifat [14] do not exceed 2%.

Table 2:
Validation of the critical frequencies obtained by our program after comparison with the theoretical and experimental results of Al-Shudeifat, in the case of an uncracked rotor [14].

Reference	Critical frequencies (Hz)					
	ω_{b1}	ω_{f1}	ω_{b2}	ω_{f2}	ω_{b3}	ω_{f3}
Our results	57.64	61.94	175.79	184.47	413.32	438.99
Al-Shudeifat's experimental results [14]	56.6	-	-	-	-	-
Al-Shudeifat's theoretical results [14]	57.8	62	176.4	184.9	414.8	438.6
Deviation ε_1 (between our results and Al-Shudeifat's theoretical results [14])	0.28	0.1	0.34	0.23	0.36	0.09
Deviation ε_2 (between our results and Al-Shudeifat's experimental results [14])	1.83	-	-	-	-	-

Table 3:
Validation of the critical frequencies obtained by our program after comparison with the theoretical and experimental results of Al-Shudeifat [14], in the case of a cracked rotor.

Reference	Critical frequency (Hz)					
	ω_{b1}	ω_{b1}	ω_{b1}	ω_{b1}	ω_{b1}	ω_{b1}
Our results	56.31	60.64	169.22	178.96	410.4	431.4
Al-Shudeifat's experimental results [14]	55.7	59.9	166.6	176	410	427
Al-Shudeifat's theoretical results [14]	-	60.7	-	-	-	-
Deviation ε_1 (between our results and Al-Shudeifat's theoretical results [14])	1.09	1.24	1.57	1.68	0.1	1.03
Deviation ε_2 (between our results and Al-Shudeifat's experimental results [14])	-	0.01	-	-	-	-

4.3. Description of the new method

The proposed new method is based on the theory of reduction in the stiffness of the cracked element (K_{crack}) as compared to that of the uncracked element ($K_{nocrack}$). This decrease may be expressed as a relation that links the two stiffnesses. The proposed method gives a set of results that allow building a database that helps to predict the presence of a crack as well as its level of severity.

The new method proposed in the present work is used to study the two most common crack models reported in the literature, namely the open and breathing cracks.

4.3.1. Study of the open crack model

In the case of a rotor with an open crack, the stiffness of the cracked element does not change while the rotor is rotating, which means that the system is linear.

Concerning a rotor with an open crack, the linear relation (8) is proposed; it relates the stiffness of the cracked element K_{crack} and that of the uncracked element $K_{nocrack}$ by a factor α that represents the percentage of stiffness reduction due to the crack. This linear relation is given as:

$$K_{crack} = \alpha \times K_{nocrack} \quad (8)$$

where: $0 < \alpha \leq 1$. If $\alpha = 0$, then there is total fracture of the cracked element; if $\alpha = 1$, there are no cracks in the element (uncracked).

The present method is based on the study of the variation of the critical frequencies of the rotor as a function of the factor α . This variation allows predicting the presence of a crack in the rotor and its level of severity.

Figure 5 displays the variation of the first backward and forward critical frequency with respect to the factor α , when the crack is located in the third element. This figure also indicates that when the factor α (the stiffness of the cracked element) decreases, the critical frequencies decrease. This decrease in stiffness is related with the crack depth.

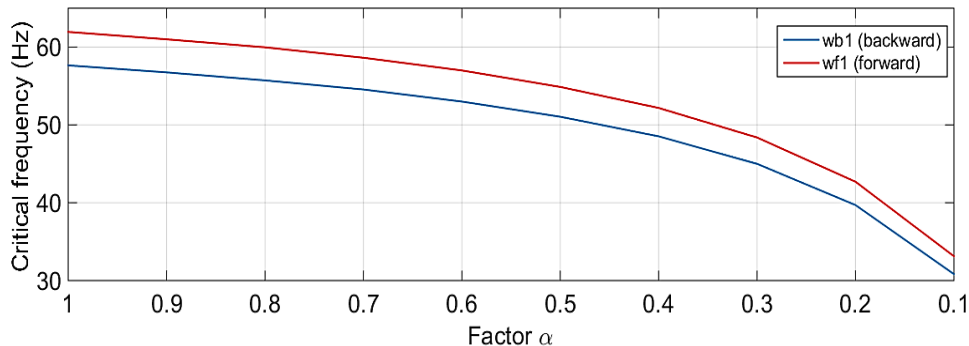


Fig.5. Variation of the first critical backward ω_{b1} and forward ω_{f1} frequencies as a function of factor α when the crack is located in the third element.

The previously stored database of critical frequencies for each value of α and each position of the crack allows us to predict the presence and the position of the crack and to estimate the crack's level of severity associated with the vibratory behaviour of the rotor, using the relative variation of the critical frequencies (9), which is defined as

$$C_i = \frac{\omega_i^{uncracked} - \omega_i^{cracked}}{\omega_i^{uncracked}} \times 100 \quad (8)$$

If $C_i = 0\%$, then there is no crack in the shaft and the rotor is stable; if $C_i > 0\%$, a crack is present in the shaft. The increase in C_i is attributed to the decrease in the critical frequencies of the rotor, which means that the stiffness of the cracked element diminishes, and the level of severity of the crack becomes very important. The rotor can break and cause irreversible damage to the system.

Figures 6 and 7 display the variations of the percentages $C_{\omega b1}$ and $C_{\omega f1}$ of the first critical frequencies as a function of the factor α . These two figures show that when the stiffness of the cracked element decreases, and the crack approaches the middle of the shaft, the crack severity level becomes very important.

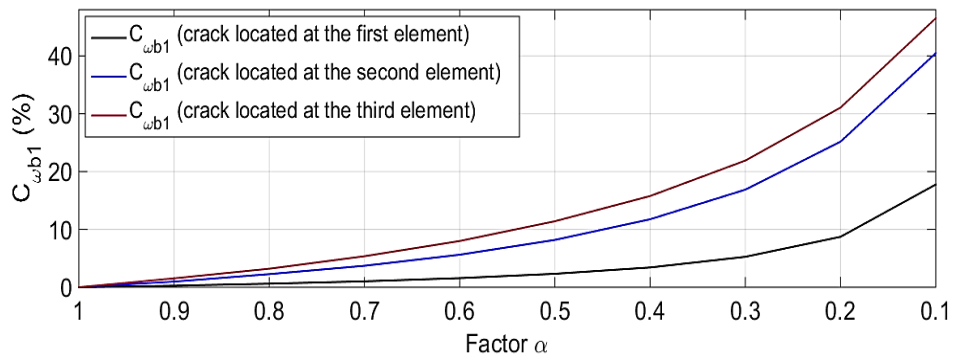


Fig. 6. Variation of the percentage $C_{\omega b1}$ of the first backward critical frequency as a function of the factor α .

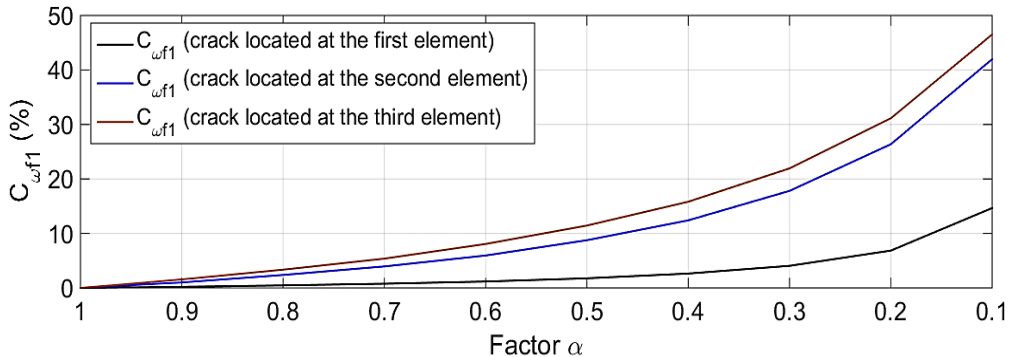


Fig. 7. Variation of the percentage $C_{\omega f1}$ of the first forward critical frequency as a function of the factor α .

4.3.2. Study of the breathing crack model

The breathing crack model is closest to the reality as compared to the other models. The crack breathing phenomenon is due to the weight of the rotor.

In the case of a rotor with a breathing crack, the stiffness of the cracked element varies during the rotation of the rotor, which means that the system is non-linear. This stiffness variation is due to the opening and closing of the crack.

To represent the variation of the stiffness of the cracked element as a function of the angle of rotation (Ωt), Al-Shudeifat et al. [11] used the function $f(\Omega t)$ which is written as:

$$f(\Omega t) = \frac{1}{2}(1 - \cos(\Omega t)) \quad (9)$$

The critical frequencies are related to the rotational angle (Ωt) as well as to the percentage of stiffness reduction α , which means that the relative variation of the critical frequencies C_i , as defined by equation (8), is also related to the rotational angle (Ωt) and the stiffness factor α .

Fig. 8 illustrates the variation of $C_{\omega b1}$ with respect to the rotational angle (Ωt), for different values of α when the crack is located in the third element. This figure indicates that, in the case of a breathing crack, C_i reaches its maximum value for the angle $\Omega t = \pi$ rad when the crack is completely open. Also $C_i = 0$ for the angle $\Omega t = 0$ rad or $\Omega t = 2\pi$ rad when the crack is completely closed. Moreover, this same figure shows that when the stiffness of the cracked element decreases, the relative variation of the critical frequencies C_i increases.

In order to check the results presented on this figure, an example is taken for the value $C_{\omega b1}$ corresponding to the case where $\alpha = 0.6$ and $\Omega t = \pi$ rad, when the crack is completely open. That value is then compared with that of a rotor with an open crack for $\alpha = 0.6$ and when the crack is located in the third element, as shown in figure 6. The two values are found practically equal on the two figures ($C_{\omega b1} \approx 8\%$).

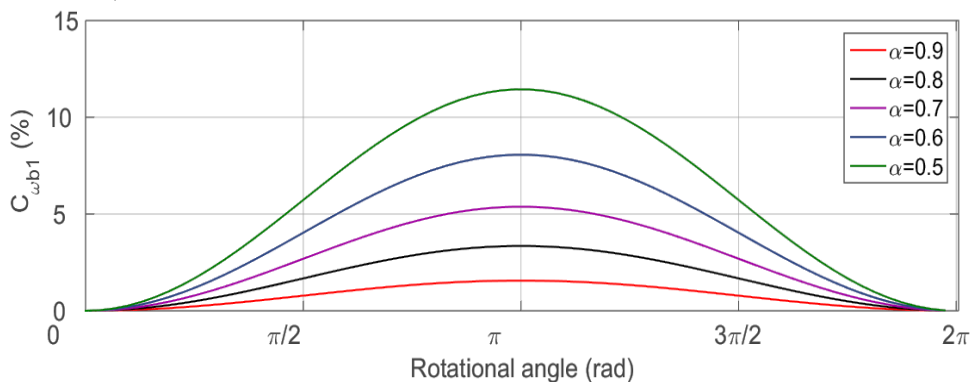


Fig. 8. Variation of $C_{\omega b1}$ with respect to the rotational angle (Ωt) for a given value of α , when the crack is located in the third element.

The curve representing the variation of the percentage C_i of the forward mode as a function of the rotational angle (Ωt) is similar to that of the backward mode.

4.3.4. Relation between the crack depth and the percentage of stiffness reduction

An attempt is made in this section to compare the variation of the critical frequencies with respect to the percentage of stiffness reduction α , and the variation of the critical frequencies with respect to the crack depth ratio μ , which is given as $\mu=h/R$, where h is the crack depth and R is the radius of the shaft; the ratio μ varies from 0 to 1. However, the opposite occurs for α varying from 1 to 0. If $\mu = 0$, then there is no crack; if $\mu = 1$, the crack depth may reach the center of the shaft.

The curves in figures 9 and 10 represent the variation of the first backward and forward critical frequency of a cracked rotor system with an open and breathing crack as a function of H , which is related to α and μ through the relations $\alpha = H$ and $\mu = 1-H$. This factor is proposed just to find similar variation curves of the frequencies.

These figures depict the graphical variation of the results obtained by the method suggested in this paper, in the case of an open cracked rotor and a breathing cracked rotor, with $Qt = \pi/2$ rad, and the theoretical results of Al-Shudeifat [14], knowing that this researcher [14] validated his theoretical results based on the experimental ones.

The graphical variation of the critical frequencies found by the suggested method is slightly similar to that obtained from Al-Shudeifat's theoretical results [14]; this researcher used the time-varying stiffness method for that purpose. It is possible to narrow the gap between our results and those of Al-Shudeifat by varying the length of the cracked element. The variation of the length has an impact on the stiffness of the cracked element as compared to that of the uncracked element.

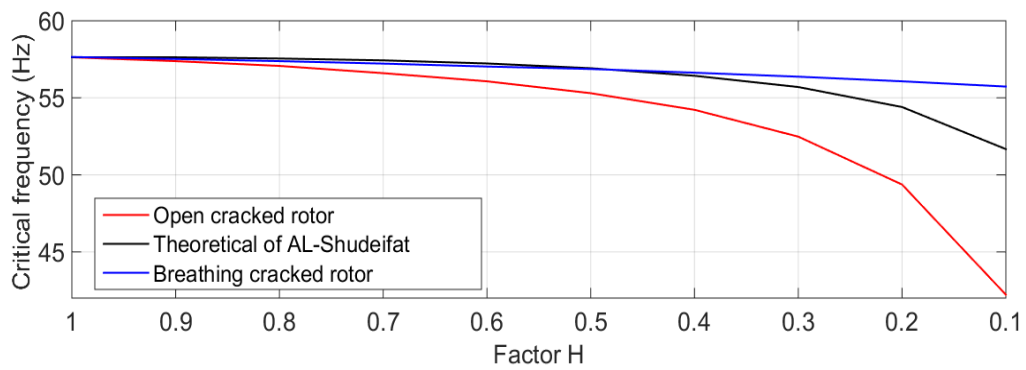


Fig. 9. Variation of the first backward critical frequency ω_{b1} as a function of the factor H , when the crack is located in the second element.

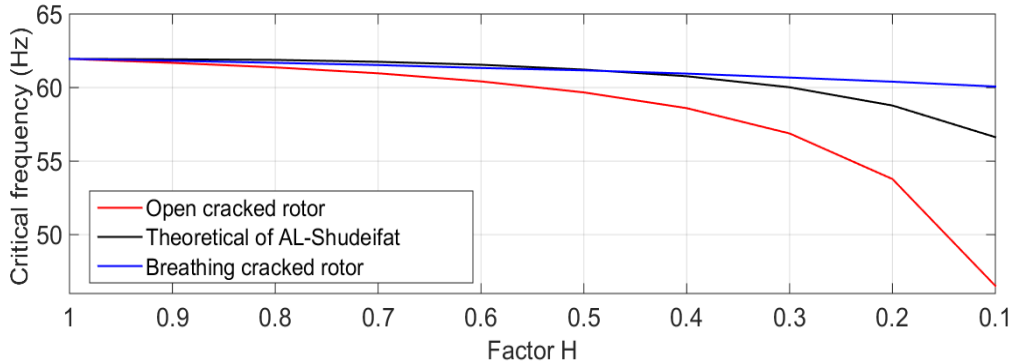


Fig. 10. Variation of the first forward critical frequency ω_{f1} as a function of the factor H, when the crack is located in the second element.

4.3.5. Influence of the variation of stiffness on the vibration amplitude of rotors

The influence of stiffness variation due to the crack on the critical frequencies of rotors has been previously studied in this work. It is not the only way to detect the presence of cracks. In this section, the effect of stiffness variation of the cracked element on the vibration amplitude of rotors is presented.

Figure 11 shows the graphical variation of the vertical amplitude with respect to the rotational speed Ω of cracked and uncracked rotors. This figure shows that the amplitude increases when the rotor approaches its critical speeds. The vibration amplitudes of cracked and uncracked rotors are different. Moreover, it is noted that the critical frequencies decrease.

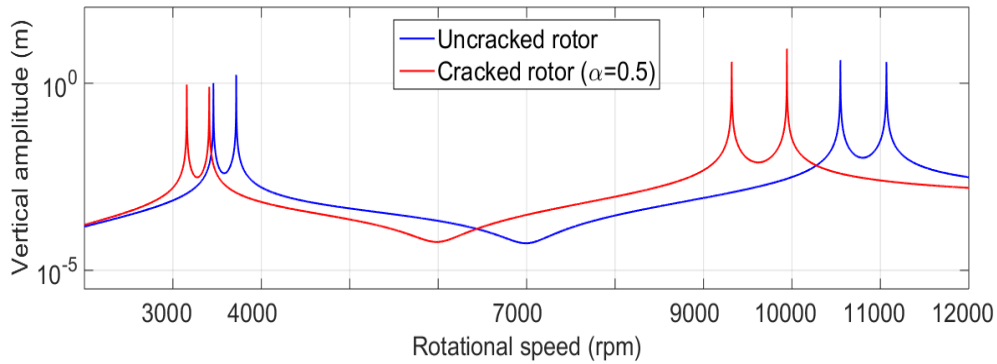


Fig. 11. Vertical amplitudes at node 6 for $\alpha=0.5$ and for mass unbalance $m_e = 6.3 \times 10^{-4} \text{ kg.m}$.

5. Conclusions

This paper attempts to propose a new method to predict the presence of cracks in the rotor's shaft. This novel method is based on the theory of stiffness

reduction in a cracked element. It is found that the crack decreases the stiffness of the cracked element as compared to the uncracked element. The cracked rotor was modeled using the classical version of the finite element method (FEM), and a program was developed under MATLAB in order to determine the critical frequencies of a cracked rotor and an uncracked rotor.

The suggested method allowed us to note that a relationship exists between the stiffness K_{crack} of a cracked element and $K_{nocrack}$ of an uncracked element. These two quantities are related by a factor α that represents the percentage of stiffness reduction. This new method can be used to study the effect of open and breathing cracks on the variation of the critical frequencies of the rotor. Based on the fluctuation of the critical frequencies, one can define the percentage C_i that represents the crack severity level.

From the results obtained by this method, it is possible to build a database that allows predicting the presence of a crack and its nature, as well as the extent of damage the crack may have on the rotor.

The findings obtained with this new method were compared with previously reported theoretical results, using the time-varying stiffness method, in order to model the crack, as given by Al-Shudeifat [14]. The results found allowed confirming the efficiency of our method in the study of cracked rotors.

R E F E R E N C E S

- [1]. *P. G. Kirmser*. "The effect of discontinuities on the natural frequency of beams". Proceedings of the American Society of Testing and Materials, **vol. 44**, 1944, pp.897–904.
- [2]. *W. J. Thomson*. "Vibration of slender bars with discontinuities in stiffness". Journal of Applied Mechanics, **vol. 16**, 1949, pp. 203-207.
- [3]. *G. R. Irwin*. "Analysis of stresses and strains near the end of a crack traversing a plate". Journal of Applied Mechanics. **vol. 24**, 1957, pp. 361–364.
- [4]. *J. Wauer*, "On the dynamics of cracked rotors: a literature survey", Applied Mechanics Review, **vol. 43**, no. 1, 1990, pp. 13–17.
- [5]. *W.G.R. Davies, I.W. Mayes*, "The vibrational behaviour of a multi-shaft, multi-bearing system in the presence of a propagating transverse crack", Journal of Vibration, Acoustics, Stress, and Reliability in Design, **vol. 106**, no. 1, 1984 , pp. 146–153.
- [6]. *A.C. Chasalevris, C.A. Papadopoulos*, "Coupled horizontal and vertical bending vibrations of stationary shaft with two cracks", Journal of Sound and Vibration, **vol. 309**, no. 3-5, Jan. 2008, pp. 507–528.
- [7]. *A.S. Sekhar*, "Vibration characteristics of a cracked rotor with two open cracks", Journal of Sound and Vibration, **vol. 223**, no. 4, Jun. 1999. pp. 497–512.
- [8]. *A.S. Sekhar, B.S. Prabhu*, "Transient analysis of a cracked rotor passing through critical speeds", Journal of Sound and Vibration, **vol. 173**, no. 3, May. 1994. pp. 415–421.
- [9]. *J. Sinou*, Effects of a crack on the stability of a non-linear rotor system, International Journal of Non-Linear Mechanics, **vol. 42**, no. 7, Sept. 2007, pp. 959–972.
- [10]. *J. Sinou, A.W. Lees*, "The influence of cracks in rotating shafts", Journal of Sound and Vibration, **vol. 285**, no. 4-5, Aug. 2005, pp. 1015–1037.

- [11]. *M.A. AL-Shudeifat, E.A. Butcher, C.R. Stern*, “General harmonic balance solution of a cracked rotor-bearing-disk system for harmonic and sub harmonic analysis: analytical and experimental approach”, International Journal of Engineering Science, **vol. 48**, no. 10 , Oct. 2010, pp. 921–935.
- [12]. *M.A. AL-Shudeifat, E.A. Butcher*, “New breathing functions for the transverse breathing crack of the cracked rotor system: approach for critical and subcritical harmonic analysis”, Journal of Sound and Vibration, **vol. 330**, no. 3, Jan. 2011, pp. 526–544.
- [13]. *M.A. AL-Shudeifat*, “On the finite element modeling of an asymmetric cracked rotor”, Journal of Sound and Vibration, vol. 332, no. 11, May. 2013, pp. 2795–2807.
- [14]. *M.A. AL-Shudeifat*, “Stability analysis and backward whirl investigation of cracked rotors with time-varying stiffness”. Journal of Sound and Vibration, vol. 348, July. 2015, pp. 365–380.